DOI: *https://doi.org/10.31351/vol34iss3pp162-172*

Improvement of Solubility and Dissolution of Niclosamide using Metal Organic Framework 5 (MOF-5)

Hayder Yahya Mansoor Al-Jarsha[1] and Mowafaq M. Ghareeb[*1]

[1]Department of pharmaceutics, College of pharmacy, University of Baghdad, Baghdad, Iraq.

[*]**Corresponding author**

Received 13/3/2024, Accepted 19/5/2024, Published 20/9/2025

Abstract

Metal-organic frameworks-5 (MOF-5) was explored for the enhancement of the solubility and dissolution of the drug niclosamide (NIC). MOF-5 was synthesized by the solvothermal method and NIC was loaded into it (NIC@MOF-5). Characterization was done using field-emission scanning electron microscopy (FE-SEM), X-ray diffraction (XRD), Fourier transform infrared spectroscopy (FTIR), Brunauer-Emmett-Teller surface area (BET-SA), and energy-dispersive X-ray spectroscopy (EDS). The effect of loading time on the percentages of entrapment efficiency (%EE) and loading capacity (%LC) were studied. The effect of incorporation into MOF-5 on saturated solubility and dissolution profiles of NIC was investigated in three different media: acidic buffer solution (ABS) pH 1.2, deionized water (DW) pH 6.2, and phosphate buffer solution (PBS) pH 7.4. The results showed that the solubility of NIC was significantly improved upon incorporation into MOF-5 in all media. In ABS pH 1.2, it was improved by 3.4 times (10.63 ± 1.04 µg/ml versus 3.17 ± 0.55 µg/ml). In DW pH 6.2, it was improved by 4.7 times (60.37 ± 4.74 µg/ml versus 12.83 ± 1.76 µg/ml). The biggest improvement was in PBS pH 7.4 by 6.1 times (209.85 ± 9.77 µg/ml versus 34.5 ± 1.66 µg/ml). For dissolution, the cumulative release at the end of point was significantly higher for NIC@MOF-5 in all three media: 51.20% ± 6.52% versus 10.77% ± 1.78% in ABS pH 1.2, 54.09% ± 1.81% versus 12.44% ± 0.57% in DW pH 6.2, and 84.87% ± 9.99% versus 19.48% ± 1.82% in PBS pH 7.4. Characterization confirmed the identity of NIC and MOF-5 as well as loading of NIC into MOF-5 without significant interactions. It is, therefore, concluded that MOF-5 is a feasible formulation approach to improve the solubility and dissolution of NIC in either acidic media, water, or basic media.

Keywords: Dissolution, improvement, MOF-5, niclosamide, solubility.

Introduction

Most of the novel medications that come out of drug development programs have relatively poor water solubility properties, which lead to poor oral bioavailability due to inadequate gastrointestinal tract dissolution [1, 2]. One of the biggest challenges facing scientists working on pharmaceuticals is finding methodologies to get over this obstacle and permit oral delivery of these novel chemical entities. Although a number of formulation strategies, including nanotechnology, emulsion-based systems, and solid dispersions, have produced encouraging results; there are still relatively few commercial uses for these technologies. This highlights the necessity to research new types of strategies along with the rise in the prevalence of new poorly water-soluble drugs [3].

Recently, metal organic frameworks (MOFs) have attracted considerable attention due to their high potential for enormous applications. Since their first appearance in the 1990s, they have been successfully investigated in several sectors, such as gas separation and storage , catalysis , sensing, storage of energy, separation and purification, harvesting of water, electronics and optoelectronics, and agriculture. In the field of drug delivery, MOFs have been examined for drug encapsulation, controlled release, targeted delivery, delivery of genes, combination of therapeutics, and therapeutic gas delivery [4].

Improving solubility is a high-potential application of MOFs. Suresh et al [5] successfully enhanced both the solubility and dissolution of triamterene, curcumin, and sulindac by MOF-5, which inhibited crystallization of the entrapped amorphous phase and subsequently the release of medication by irreversible collapse of MOF-5 structure. Ohsaki et al [6] utilized ZIF-8 to improve solubility of indomethacin which was also attributed to the surface deposition of the amorphous form of the drug on the ZIF-8 particles. Bajaj et al [7] reported an enhancement of solubility of mebendazole after incorporation within ZIF-8. Chen et al used cyclodextrin metal-organic framework (CD-MOF) to enhance solubility of isosteviol. Nano sized CD-MOF cages were also reported by He et al [8] to

improve the solubility and bioavailability of azilsartan. Han et al. [1] managed to improve the solubility of ketoprofen, Ibuprofen, and felodipine, using HKUST-1/ graphite oxide matrix. NIC is an anthelmintic drug approved for infections caused by *Taenia saginata* (beef tapeworm), *Taenia solium* (pork tapeworm), *Diphyllobothrium latum* (fish tapeworm), and *Hymenolepis nana* (dwarf tapeworm) [9].

Several pharmacological screenings have revealed it to be a highly promising molecule with a potential for treatment of malignancies, bacterial infections, type II diabetes, arterial constriction, rheumatoid arthritis, endometriosis, as well as a wide spectrum of viral infections [10-12]. NIC is classified by biopharmaceutics classification system as class II medication with low solubility, and low permeability which restricts its oral absorption [13]. The use of NIC in clinical indications other than anthelmintic has been attempted. A noticeable phase I clinical trial in the USA for using NIC in combination with enzalutamide in men with castration-resistant prostate cancer [14]. The trial was terminated as the plasma concentration of tolerable dose did not provide adequate plasma concentrations proposed for tumor growth inhibition. Accordingly, there is an unmet need to increase the solubility and dissolution rate of NIC, hence its bioavailability and effectiveness in this and other potential indications.

Efforts have been made to increase bioavailability of NIC. These include formation of co-crystals [15], solid lipid nanoparticles [16], dendrimer-like structures [17], micelles [18], nanosuspensions [19], chitosan nano cargos [20], lipid emulsions [21], and nanocrystals [22]. In the present study, MOF-5 was investigated to improve the solubility of NIC. MOF-5 undergoes hydrolysis in water due to cleavage of its coordination bonds. MOF-5, with the chemical formula Zn4O(BDC)3; BDC = 1,4-benzodicarboxylate, is a water soluble MOF. The cubic, porous framework is built from [Zn4O]+6 clusters of zinc and linked through BDC-2 ligands [23]. Zinc is a relatively safe metal (lethal dose (LD50) ≈ 3 g/kg) that is widely used in nutritional supplements either as zinc acetate, zinc oxide, or zinc gluconate [24]. BDC (also known as terephthalic acid) is an organic linker that also displays low toxicity and has a high safety profile when used orally (LD > 1 g/kg in mouse models) [25]. The MOF-5 structure also shows a relatively large pore size of approximately 12.5 Å in diameter, making it appropriate for accommodating small-molecule drugs [5], like NIC.

Materials and Methods

NIC was purchased from Hangzhou Hyper Chemicals Limited, China. Zinc nitrate hexahydrate ($Zn(NO_3)_2.6H_2O$) was obtained from Central Drug House, India. 1,4-benzene dicarboxylic acid (H_2BDC) was bought from Reagent World, USA. Ethanol, chloroform and dimethyl formamide (DMF) were obtained from Alpha Chemika, India.

Synthesis of MOF-5

The synthesis of MOF-5 was carried out by the conventional solvothermal method described in our previous work [26] . In short, 50 ml of DMF were used to dissolve 0.39 g of BDC and 2.16 g of $Zn(NO_3)_2.6H_2O$. The mixture was then stirred for 30 minutes to ensure the solvation of the ingredients. After that, the solution was put into a polytetrafluoroethylene-lined 100-ml solvothermal reactor (Xiamen Ollital Technology Co., Ltd.) and heated for 60 hours at 130 °C using an oven (DZ-1BC, Faithful Instruments). Then, the reactor was left to cool to ambient temperature, the mixture was centrifuged at 4000 rpm, and the solid was recovered by decantation and washed two times with DMF. Following that, the solvent was exchanged with chloroform for the next three days, with fresh chloroform replaced every day. The produced powder was dried under vacuum at 80 °C by applying a dynamic vacuum in the oven used, and stored in a degassing chamber (1.2 L, Bacoeng).

Activation and loading of MOF-5 with NIC

The activation of MOF-5 was done in the dynamic vacuum oven. The temperature used was 70 °C for 12 hours, followed by 120 °C for another 12 hours. This step is crucial to ensure removal of any residual solvents and make pores available for loading. The simple agitation approach was used to incorporate NIC into MOF-5 [5]. Solutions of 5 mg/ml were prepared for NIC in ethanol. Each solution has a volume of 30 ml. The solutions were placed into screw-capped glass vials and 100 mg of freshly activated MOF-5 were added to each of them. The vials were shaken for 2, 4, 6, 8, or 10 days using an orbital shaker (RT-202, Triup International Corp.). After that, each mixture was poured into a beaker, and part of the supernatant from each solution was stored to be used in the determination of the drug content, the obtained MOF-5 loaded with NIC (NIC@MOF-5) were washed three times with ethanol, dried at 80 °C, and stored in the vacuum chamber. Similarly, the same quantities of activated MOF-5 were placed into ethanol alone (without NIC), put onto the orbital shaker for its corresponding period, dried at 80 °C, and stored in a vacuum chamber. These were used later as control MOF-5 for evaluation of solubility and dissolution (i.e., used in physical mixtures (PM)). For each prepared solution or mixtures above, two other replicates were made so that all experiments were done in triplicates.

Characterization of MOF-5 and NIC@MOF-5

Field emission scanning electron microscopy (FE-SEM)

To determine particle size, shape, and general surface characteristics, FE-SEM images were obtained for the prepared MOF-5 and NIC@MOF-5. The imaging was performed under

1.25 x 10^{-2} Pa pressure at 30 kV [27] (Inspect F50, Field Electron and Ion Company). The images were processed with computer software (ImageJ version 1.53t, National Institute of health).

Fourier transform infrared spectroscopy (FTIR)

The FTIR spectra were obtained via KBr disc methodology between 4000 and 400 cm^{-1} at room temperature by a spectrometer FTIR-7600, Lambda Scientific Systems, Inc [28]. FTIR was obtained for MOF-5, NIC, PM, and NIC@MOF-5.

Powder X-ray diffraction (XRD)

XRD was performed for MOF-5, NIC, PM, and NIC@MOF-5. XRD diffractograms were obtained using a diffractometer (DX-2700BH, Dandong Haoyuan Instrument) with a copper Kα radiation source (30 kV and 20 mA) and λ = 1.54056 Å. The range of scanning of 2-theta (2θ) was 5 – 50 degrees [26, 29].

Brunauer-Emmett-Teller surface area (BET-SA) analysis

The pore volumes and surface areas were obtained by nitrogen adsorption/desorption at 77 K using a surface area analyzer (ASAP 2020, Micromeritics Instrument Corporation). A vacuum drying oven was used in the activation of MOF-5 [30]. The activation was done at 70 °C for 12 hours, followed by 120 °C for another 12 hours under a dynamic vacuum. The analysis was done for MOF-5 and NIC@MOF-5.

Energy-dispersive X-ray spectroscopy (EDS)

To assess the chemical composition of MOF-5, EDS was performed at an acceleration voltage of 30 kV [31] using Axia ChemiSEM, Thermo Fisher Scientific, Netherlands.

Drug content, entrapment efficiency, and loading capacity.

Supernatants collected from incorporation solutions were used to calculate the drug content loaded into MOF-5. After appropriate dilutions, the concentrations were determined spectrophotometrically at 333 nm from a previously established calibration curve using UV-Vis spectrophotometer (UV-VIS1900i Shimadzu Corporation, Japan). From these concentrations, the quantities remaining in the solution were determined. By subtracting these remaining quantities from the original quantity of NIC that was used for incorporation, the weights of NIC enclosed within MOF-5 were calculated [32, 33].

The calculation of percentage of entrapment efficiency (%EE) was done using the equation below:

$$\%EE = \frac{\text{Weight of drug entrapped by MOFs}}{\text{Total weight of drug}} \times 100$$ …… Equation. 1 [34]

Percentage loading capacity (%LC) was then calculated as:

$$\%LC = \frac{\text{Weight of drug entrapped by MOFs}}{\text{Weight of MOFs+weight of drug entrapped by MOFs}} \times 100$$ …… Equation. 2 [34]

Determination of solubility

The solubility was examined by simple shake-flask method [35] in three different media: ABS pH 1.2, DW pH 6.2, and PBS pH 7.4. Three replicates of each of NIC drug powder, NIC@MOF-5 or PM of NIC and MOF-5 were put in excess into screw-capped glass vials containing their corresponding medium and then shaken for 72 hours using an orbital shaker. The mixtures were then centrifuged at 4000 rpm, the supernatants were then filtered by syringe filter (0.45 μm), and the concentrations of NIC were determined spectrophotometrically [7].

In vitro drug release

The release of NIC from NIC@MOF-5, from its PM with MOF-5, and from the marketed product of NIC (Yomesan®, Beyer AG) was performed using a paddle type USP dissolution apparatus (RC-6, Faithful Instruments) at 50 rpm. The release was performed in triplicates at 37 °C in 900 ml of either ABS pH 1.2, DW pH 6.2, or PBS pH 7.4. The equivalent quantity of NIC was 250 mg. The dissolution was carried out for 6 hours. 10% ethanol was added to maintain sink conditions. Samples of 5 ml were withdrawn (at 5, 10, 20, 30, 60, 120, 180, 240, and 360 minutes) with replenishment of volumes with fresh medium. Samples were filtered through a 0.22 μm filter and their concentrations were determined spectrophotometrically [6, 36, 37].

Statistical analysis

Analysis of variance (ANOVA) was performed using Minitab® statistical software version 21.2 (2022).

Results and Discussion

Characterization of MOF-5 and NIC@MOF-5

FE-SEM

A white crystalline of MOF-5 powder was obtained and is similar in general appearance to the described MOF-5 in the literature [38]. FE-SEM images of MOF-5 are shown in Figure 1. The surface of MOF-5 was smooth and had a high number of tunnels of different opening sizes (Figure 1: B and C). Figure 1: D also shows that all outer and inner surfaces had nano-sized pores (white and red arrows, respectively). The size of these pores ranged from 15 x 40 nm to 403 x 44 nm. The high number of tunnels and enormous pores in prepared MOF-5 accounts for its porous structure and huge surface area. This makes MOF-5 capable of accommodating small-sized drug molecules [5] (like NIC).

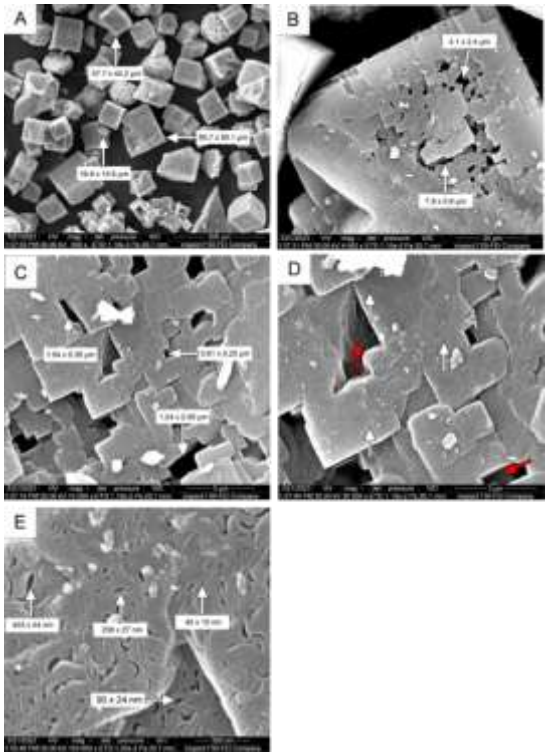

Figure 1. FE-SEM images of MOF-5 showing general field and size of cubes [A], size of tunnel openings [B and C], nano-sized pores [E], and sizes of pores [E].

Upon incorporation of NIC into MOF-5, the powder changed in color to brownish. FE-SEM images of NIC @MOF-5 are displayed in Figure 2. Since NIC is incorporated inside the MOF-5, no NIC molecules were seen within the bulk or at large pore opening. However, a reduction in the number of some surface pores, especially the nano-sized surface pores seen in Figure 1: D and E versus Figure 2: D and E). Some NIC might be responsible for this as NIC can clog the nano-sized surface pores, making them disappear in the imaging.

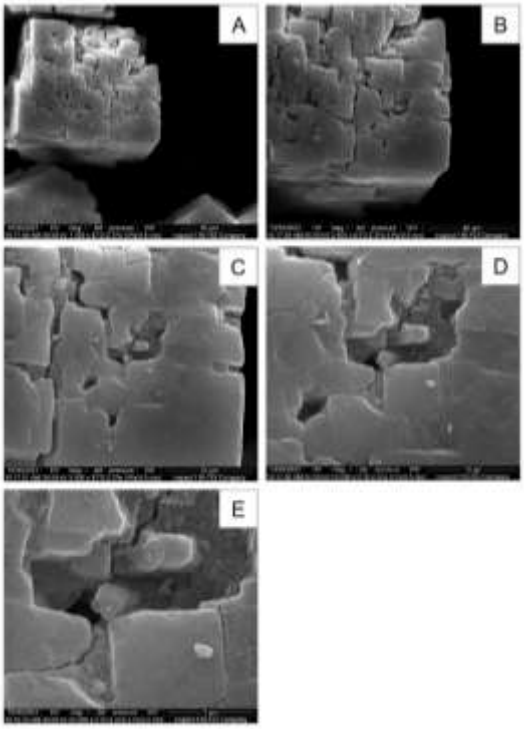

Figure 2. FE-SEM images of NIC@MOF-5 showing general view [A, B, and C], and reduced pores on surface [D and E].

FTIR and XRD

Figure 3 and Figure 4 show FTIR spectra and XRD diffractograms of NIC, MOF - 5, NIC@MOF-5, and PM.

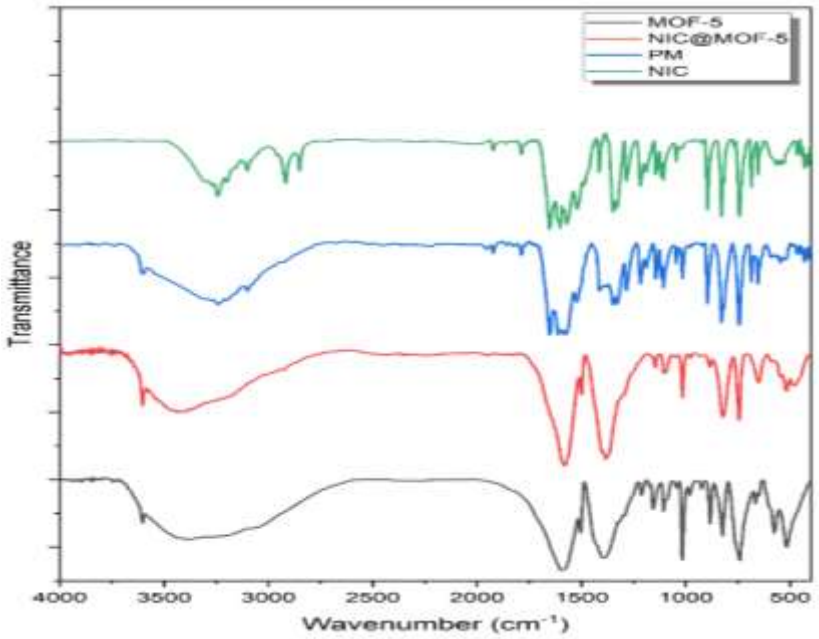

Figure 3. FTIR spectra of NIC, MOF-5, NIC@MOF-5, and PM (of NIC and MOF-5).

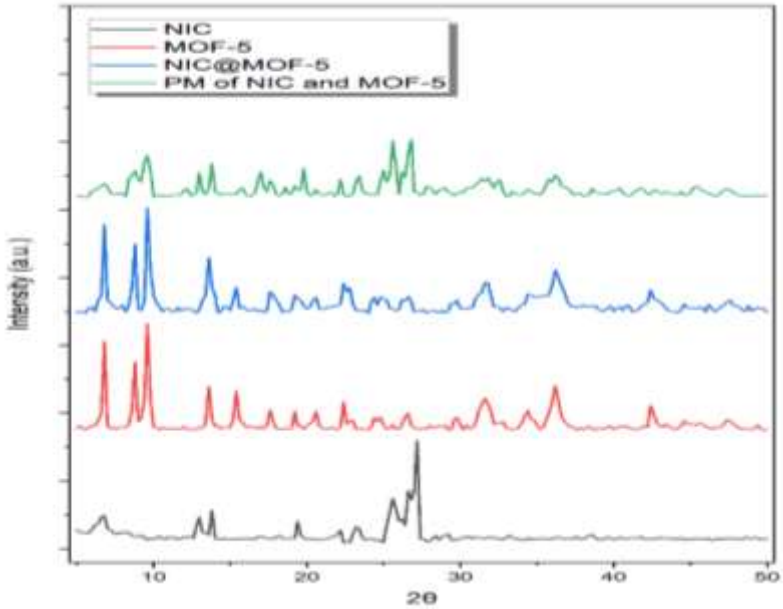

Figure 4. XRD diffractograms of NIC, MOF-5, NIC@MOF-5, and PM.

The XRD diffractogram and FTIR spectrum of NIC@MOF-5 were shown to be similar to that of MOF-5. Additionally, the PM showed a mixtures of peaks of NIC and MOF-5. This confirms that the drug is incorporated inside the pores of MOF-5 with no residue on the surface or within the bulk of the mixture. In addition, if potential interaction existed between NIC and MOF-5 within the NIC@MOF-5, it would change the peaks of NIC@MOF-5 compared to MOF-5. As no significant alteration took place, this can reflect absence of such interaction [7, 8].

BET-SA analysis

Drugs can occupy and close the pores inside the porous structure of MOFs, hence decreasing the MOFs' original high SA. More or larger molecules result in a higher drop in accessible SA within the MOF. The amount and type of the molecules loaded determine how much of a loss in surface area and pore volume takes place [6, 39].

Table 1 displays the surface areas and pore volumes of MOF-5 and NIC@MOF-5.

Table 1. Surface areas and pore volumes of MOF-5 and NIC@MOF-5.

	BET-SA (m^2/g)	Pore volume (cm^3/g)
MOF-5	800.0	0.369
NIC@MOF	8.4	0.028

When comparing BET-SA and the pore volume of NIC@MOF-5 versus MOF-5, a dramatic reduction is seen in both. This confirms that NIC filled the pores of MOF-5 and/or closed its pore openings.

EDS

The EDS spectrum of the prepared MOF-5 (Figure 5) showed absorption bands with peaks at 1.0, 8.6, and 9.6 keV, indicating a typical zinc metallic absorption. It also showed typical peaks of O and C at 0.5 and 0.26 keV, respectively. The composition analysis of the prepared MOF-5 was comparable to the previously reported MOF-5 [40].

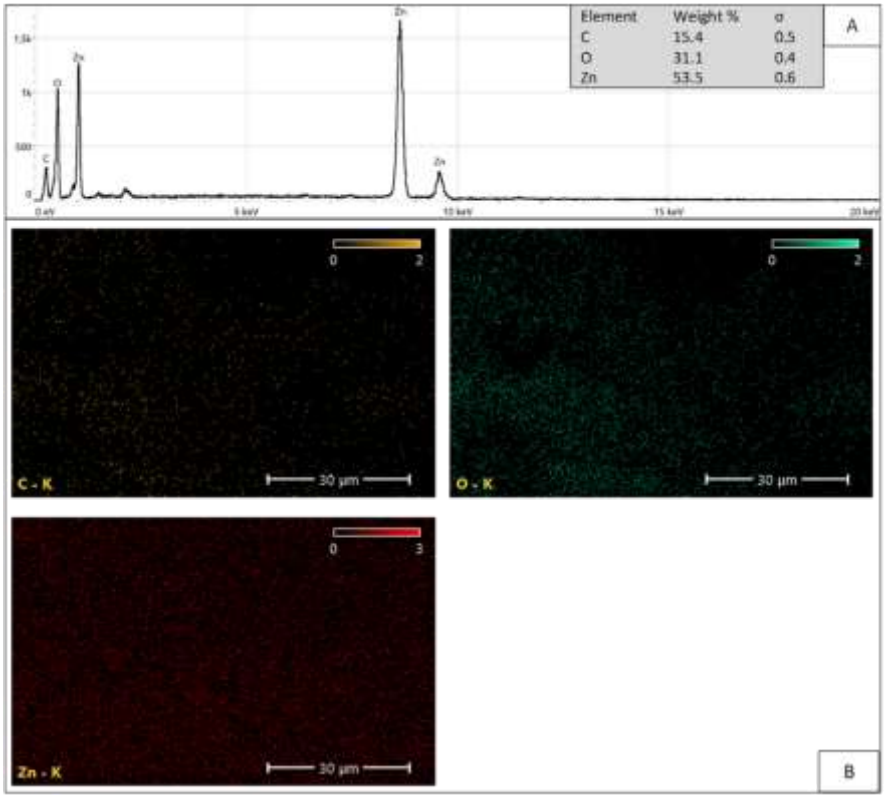

Figure 5. (A) EDS and (B) elemental mapping of the synthesized MOF-5.

Drug content, entrapment efficiency, and loading capacity

Figure 6 shows the effect of duration of shaking in orbital shaker on %EE and %LC. ANOVA between each two sequential points on each curve showed that increasing the duration significantly increased both %EE and %LC between 2 and 8 days ($P < 0.05$). However, there was no significant difference between 8 and 10 days ($P > 0.05$). Several durations have been reported in literature for the duration of incorporation of drugs into MOFs. Ohsaki et al. [6] and Al Haydar et al. [41] took 24 hours to incorporate indomethacin and ibuprofen into MOFs, respectively. Loading MOF-5 with oridonin by Chen et al. [42] took 72 hours. Suresh et al. [5] spent 6 days to incorporate triamterene and 10 days for each of curcumin and sulindac into MOF-5. Initially, as the agitation begins, the drug diffuses into the MOF's pores, increasing the amount of drug loaded. Because of MOF's limited capacity, this rise can only continue for a limited time. Upon reaching a saturation stage where the drug has filled all the available pores, further shaking does not enhance the drug loading. This stage results from the system reaching equilibrium, when the rate of drug entering the pores matches the rate of any drug exiting the pores, and there is no longer any room within the MOF for the drug to occupy.

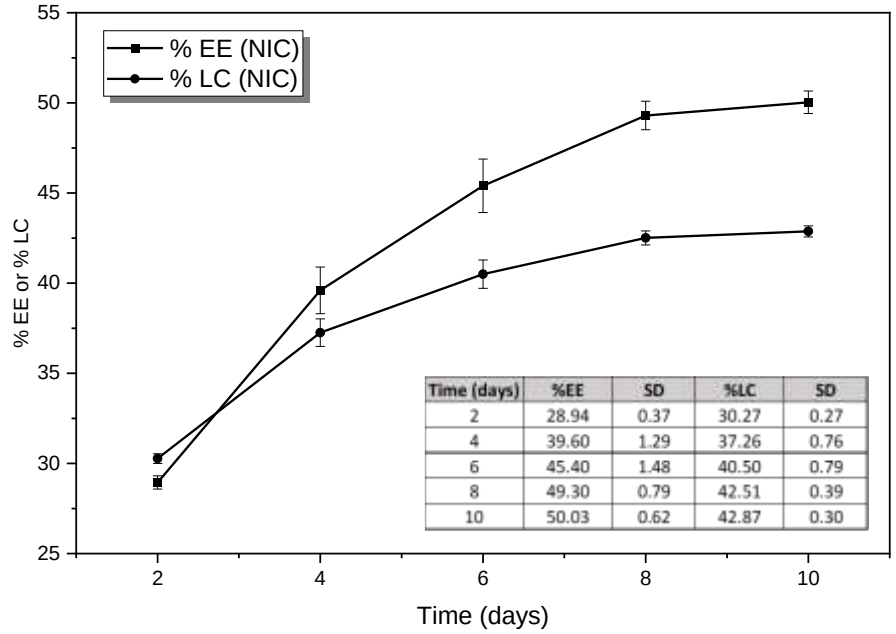

Time (days)	%EE	SD	%LC	SD
2	28.94	0.37	30.27	0.27
4	39.60	1.29	37.26	0.76
6	45.40	1.48	40.50	0.79
8	49.30	0.79	42.51	0.39
10	50.03	0.62	42.87	0.30

Figure 6. The effect of duration of shaking on %EE and %LC of NIC.

Determination of solubility

Table 2 shows the solubility values obtained for NIC alone as powder as well as from PM and NIC@MOF-5 in the three media under investigation. No significant differences were found between the solubilities of NIC as a powder and PM ($P > 0.05$). On the other hand, NIC showed significantly higher solubility from NIC@MOF-5 compared to its PMs in the three media under investigation (ANOVA P values < 0.001). The highest improvement reached was about 6 times in PBS pH 7.4 followed by about 5 times improvement in DW pH 6.2. The lowest improvement for NIC was about 3.5 times in ABS pH 1.2.

Table 2. Solubilities (µg/ml) of NIC (powder) and from PM and NIC@MOF-5 in different media

Medium	NIC	PM	NIC@MOF-5
ABS pH 1.2	3.17 ± 0.55	3.03 ± 0.21	10.63 ± 1.04
DW pH 6.2	12.83 ± 1.76	12.25 ± 1.28	60.37 ± 4.74
PBS pH 7.4	34.5 ± 1.66	33.67 ± 2.58	209.85 ± 9.77

MOFs can improve solubility of drugs by two main mechanisms. The most apparent one is by increased rate of dissolution brought by SA improvement and particle size reduction. The rapid collapse of MOF-5 structures once in contact with aqueous media allows instant release of nanometer-sized particles having a very high contact surface area with the vehicle. This, besides improving the wettability of the drug molecule, significantly improves its solubility. Bajaj et al [7] reported improvement in saturated solubility of mebendazole via MOFs and the enhancement was attributed to the particle size reduction and improved wettability. The improvement of NIC was likely due to this mechanism.

Comparing the solubility of NIC from drug powder alone or from NIC@MOF-5 in different media, significant differences exist between ABS pH 1.2, DW pH 6.2, and PBS pH 7.4 ($P < 0.001$). This is anticipated and aligned with the reported nature of NIC as it has a pH dependent solubility [10].

In vitro drug release

Figure 7, Figure 8, and Figure 9 show the comparative dissolution profiles of NIC (from NIC@MOF-5, PM, and Yomesan®) in ABS pH 1.2, DW pH 6.2, and PBS pH 7.4, respectively.

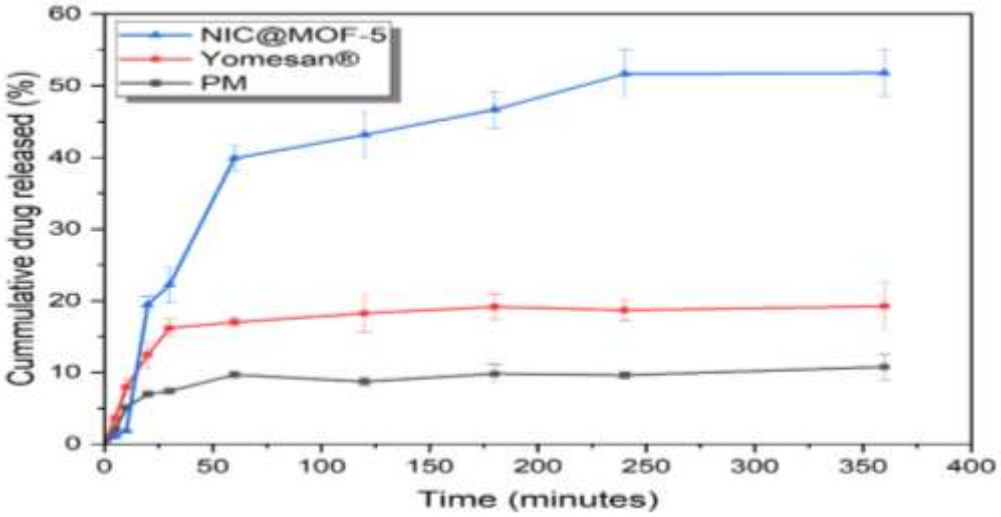

Figure 7. Comparative dissolution profile of NIC from NIC@MOF-5, PM, and Yomesan® in ABS pH 1.2.

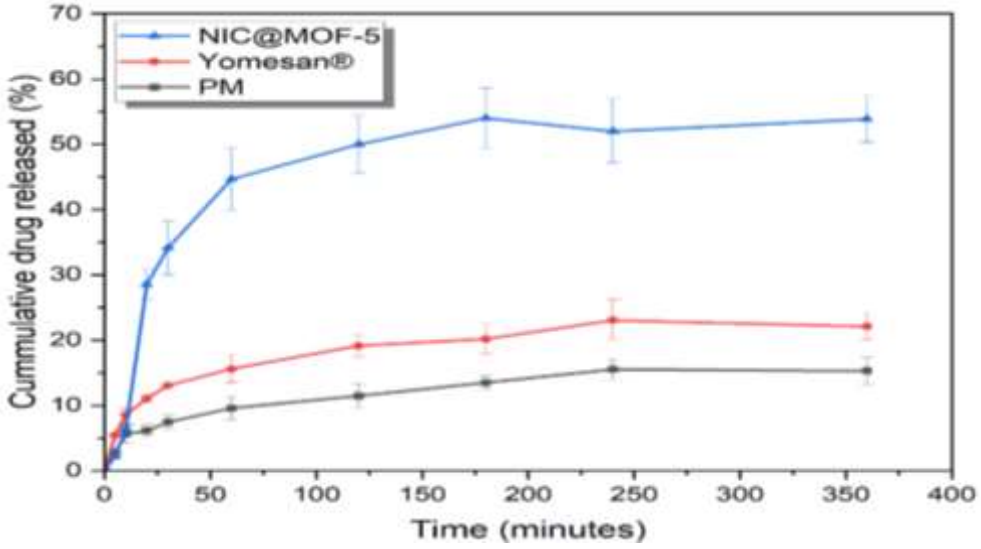

Figure 8. Comparative dissolution profile of NIC from NIC@MOF-5, PM, and Yomesan® in DW pH 6.2.

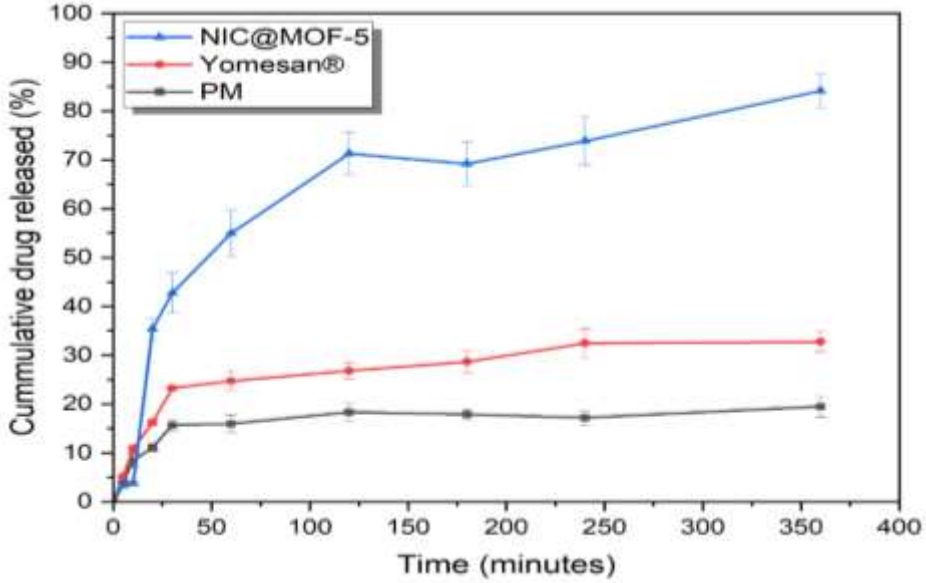

Figure 9. Comparative dissolution profile of NIC from NIC@MOF-5, PM, and Yomesan® in PBS pH 7.4.

NIC released from MOF-5 had superior ~~and~~ improvement over both PM and Yomesan® in all media. It managed to release approximately 50% of NIC in both ABS pH 1.2 and DW pH 6.2 while released 84% in PBS pH 7.4. Although the saturated solubility of NIC was significantly different between ABS pH 1.2 and DW pH 6.2, the cumulative percentages released in dissolution were not significantly different at the end points (at 360 minutes, cumulative release from NIC@MOF-5 was 51.8% ± 3.3% in ABS pH 1.2 and was 53.9% ± 3.5% in DW pH 6.2, $P > 0.05$). Two factors might contribute to this: First, the time for saturated solubility study was 72 hours as compared to the 6 hours of dissolution study. Second, the co-solvent alcohol at 10% v/v concentration was added to maintain sink conditions in dissolution and did not exist in saturated solubility studies.

In both ABS pH 1.2 and DW pH 6.2, the cumulative release from NIC@MOF-5 started to be significantly different ($P < 0.05$) from Yomesan® and PM after 30 minutes. In PBS pH 7.4, it took 20 min to be significantly different. This lag time is mostly attributed to the time required for MOF-5 crystals to start collapsing and release NIC. In PM and Yomesan®, this lag time does not exist and as NIC is not incorporated within other substance.

Besides niclosamide, Yomesan® product contains sodium lauryl sulphate and povidone as excipients [(9)]. Sodium lauryl sulphate is a surfactant and wetting agent. Povidone has a dissolution enhancer property [(43)]. This can explain why Yomesan® showed a superior release of NIC versus PM in all media.

Conclusion

Due to their weak solubility, many poorly soluble compounds (like NIC) have limited applications. Improving solubility is essential to the development of new formulation for NIC. MOF-5 not only had a relatively high drug loading capacity but also the straightforwardness and simplicity of the synthesis process. Utilizing MOF-5 as a host, the solubility and release profile of NIC in different media across different pH values were significantly enhanced. This study reinforced that MOF-5 is a valuable formulation approach to improve the solubility and dissolution of a drug candidate (NIC), which has limited solubility in either acid media, water, or basic media.

Acknowledgment

The authors extend their appreciation to Assistant Prof. Dr. Rana Th Abd Alrubaye of the Department of Chemical Engineering, College of Engineering, University of Baghdad, for her assistance provided throughout the duration of this research study.

Conflicts of Interest

There are no conflicts of interest related to this work.

Funding

None.

Ethics Statements

None provided.

Author Contribution

The authors confirm contribution to the paper as follows: Hayder Y. and Mowafaq M.; data collection: Hayder Y.; analysis and interpretation of results: Hayder Y. and Mowafaq M.; draft manuscript preparation: Hayder Y. All authors reviewed the results and approved the final version of the manuscript.

References

1. Han J, Xiao B, Le PK, Mangwandi C. Enhancement of the solubility of BS class II drugs with MOF and MOF/GO composite materials: Case studies of felodipine, ketoprofen and ibuprofen. Materials. 2023;16(4):1554-68.

2. Jaafar IS, Radhi AA. Co-amorphous system: A promising strategy for delivering poorly water-soluble drugs. Iraqi journal of pharmaceutical sciences. 2020;29(1):1-11.

3. Leuner C, Dressman J. Improving drug solubility for oral delivery using solid dispersions. European journal of pharmaceutics and biopharmaceutics. 2000;50(1):47-60.

4. Maranescu B, Visa A. Applications of metal-organic frameworks as drug delivery systems. International journal of molecular sciences. 2022;23(8):4458-76.

5. Suresh K, Matzger AJ. Enhanced drug delivery by dissolution of amorphous drug encapsulated in a water unstable metal-organic framework (MOF). Angewandte chemie. 2019;58(47):16790-4.

6. Ohsaki S, Satsuma H, Nakamura H, Watano S. Improvement of solubility of sparingly water-soluble drug triggered by metal-organic framework. Journal of drug delivery dcience and technology. 2021;63:102490.

7. Bajaj T, Singh C, Gupta GD. Novel metal organic frameworks improves solubility and oral absorption of mebendazole: Physicochemical characterization and in vitro-in vivo evaluation. Journal of drug delivery dcience and technology. 2022;70:103264.

8. He Y, Zhang W, Guo T, Zhang G, Qin W, Zhang L, et al. Drug nanoclusters formed in confined nano-cages of CD-MOF: Dramatic enhancement of solubility and bioavailability of azilsartan. Acta pharmaceutica sinica B. 2019;9(1):97-106.

9. Bayer A. Yomesan (Niclosamide) PIL: Bayer AG; 2022 [Available from: https://www.bayer.com/sites/default/files/YOMESAN_EN_PI.pdf.

10. Needham D. The pH dependence of niclosamide solubility, dissolution, and

morphology: Motivation for potentially universal mucin-penetrating nasal and throat Sprays for COVID19, its variants and other viral infections. Pharmaceutical research. 2022;39(1):115-41.

11. Kapale SS, Chaudhari HK. Niclosamide and challenges in chemical modifications: A broad review on enhancement of solubility. Journal of the indian chemical society. 2021;98(12):100262.

12. Chen W, Mook RAJ, Premont RT, Wang J. Niclosamide: Beyond an antihelminthic drug. Cellular signalling. 2018;41:89-96.

13. Jara MO, Warnken ZN, Williams RO. Amorphous solid dispersions and the contribution of nanoparticles to in vitro dissolution and in vivo testing: Niclosamide as a case study. Pharmaceutics. 2021;13(1):97-111.

14. Schweizer MT, Haugk K, McKiernan JS, Gulati R, Cheng HH, Maes JL, et al. A phase I study of niclosamide in combination with enzalutamide in men with castration-resistant prostate cancer. PloS one. 2018;13(6):e0198389.

15. Grifasi F, Chierotti MR, Gaglioti K, Gobetto R, Maini L, Braga D, et al. Using salt cocrystals to improve the solubility of niclosamide. Crystal growth & design. 2015;15(4):1939-48.

16. Rehman MU, Khan MA, Khan WS, Shafique M, Khan M. Fabrication of niclosamide loaded solid lipid nanoparticles: In vitro characterization and comparative in vivo evaluation. Artificial cells, nanomedicine, and biotechnology. 2018;46(8):1926-34.

17. Xie Y, Yao Y. Octenylsuccinate hydroxypropyl phytoglycogen enhances the solubility and in-vitro antitumor efficacy of niclosamide. International journal of pharmaceutics. 2018;535(1-2):157-63.

18. Russo A, Pellosi DS, Pagliara V, Milone MR, Pucci B, Caetano W, et al. Biotin-targeted Pluronic(®) P123/F127 mixed micelles delivering niclosamide: A repositioning strategy to treat drug-resistant lung cancer cells. International journal of pharmaceutics. 2016;511(1):127-39.

19. Costabile G, d'Angelo I, Rampioni G, Bondì R, Pompili B, Ascenzioni F, et al. Toward repositioning niclosamide for antivirulence therapy of Pseudomonas aeruginosa lung infections: Development of inhalable formulations through nanosuspension technology. Mol Pharm. 2015;12(8):2604-17.

20. Naqvi S, Mohiyuddin S, Gopinath P. Niclosamide loaded biodegradable chitosan nanocargoes: An in vitro study for potential application in cancer therapy. Royal society open science. 2017;4(11):170611.

21. Zhang X, Zhang Y, Zhang T, Zhang J, Wu B. Significantly enhanced bioavailability of niclosamide through submicron lipid emulsions with or without PEG-lipid: A comparative study. Journal of microencapsulation. 2015;32(5):496-502.

22. Ye Y, Zhang X, Zhang T, Wang H, Wu B. Design and evaluation of injectable niclosamide nanocrystals prepared by wet media milling technique. Drug development and industrial pharmacy. 2015;41(9):1416-24.

23. Kaye SS, Dailly A, Yaghi OM, Long JR. Impact of preparation and handling on the hydrogen storage properties of Zn_4O(1,4-benzenedicarboxylate)$_3$ (MOF-5). Journal of the american chemical society. 2007;129(46):14176-7.

24. Plum LM, Rink L, Haase H. The essential toxin: Impact of zinc on human health. International journal of environmental research and public health. 2010;7(4):1342-65.

25. Sheehan RJ. Terephthalic acid, dimethyl terephthalate, and isophthalic acid. In: Ullmann F, Gerhartz W, Yamamoto YS, Campbell FT, Pfefferkorn R, Rounsaville JF, editors. Ullmann's encyclopedia of industrial chemistry. 26. 7th ed: Weinheim, Germany: Wiley-VCH; 2011. p. 193-217.

26. Al-Jarsha H, Ghareeb M. Application of Taguchi orthogonal array in optimization of the synthesis and crystallinity of metal-organic framework-5 (MOF-5). Tropical journal of pharmaceutical research. 2023;22(12):2473-82.

27. Kareem RA, Naji GA-H. Natural preparation of rice husk-derived silica and eggshell-derived calcium carbonate composite as a coating material for dental implant. Journal of baghdad college of dentistry. 2022;34(1):1817-69.

28. Jassim ZE, Al-Kinani KK, Alwan ZS. Preparation and evaluation of pharmaceutical cocrystals for solubility enhancement of dextromethorphan HBr. International journal of drug delivery technology. 2021;11(4):1342-9.

29. Jassim NM, Abed ZA, Mahdi ZS. Synthesis, characteristics and study the photoluminscience of the CdS_xSe_{1-x} nanocrystaline thin film. Baghdad science journal. 2020;17(1):116-9.

30. Alhussainy JM, Alrubaye RT. Gas adsorption and storage at metal-organic frameworks. Journal of engineering. 2022;28(1):65-75.

31. Abdulrahman HA, Alias MFA. Synthesis and Characterizationof a Nano$(CdO)_{0.94}$:$(In2O3)_{0.06}$/ Si gas Sensor. Iraqi journal of science. 2021;22(11):3858-70.

32. Jithan A, Madhavi K, Madhavi M, Prabhakar K. Preparation and characterization of albumin nanoparticles encapsulating curcumin intended for the treatment of breast cancer. Int J Pharm Investig. 2011;1(2):119-25.

33. Al-Sarraf MA, Hussein AA, Al-Kinani KK. Formulation, characterization, and optimization of zaltoprofen nanostructured lipid carriers (NLCs). International journal of drug delivery technology. 2021;11(2):434-42.

34. Bhattacharyya S, Reddy P. Effect of surfactant on azithromycin dihydrate loaded stearic acid solid lipid nanoparticles. Turkish journal of pharmaceutical sciences. 2019;16(4):425-31.

35. Hu M, Li X. Oral bioavailability and drug delivery: From basics to advanced concepts and applications. New Jersey, USA: John Wiley & Sons, Inc.; 2024.

36. Luedeker D, Gossmann R, Langer K, Brunklaus G. Crystal engineering of pharmaceutical co-crystals: "NMR crystallography" of niclosamide co-crystals. Crystal growth & design. 2016;16(6):3087-100.

37. Jabir SA, Sulaiman HT. Preparation and characterization of lafutidine as immediate release oral strip using different type of water-soluble polymer. International journal of applied pharmaceutics. 2018;10(5):249-60.

38. Isaeva VI, Kustov L. Metal organic frameworks—New materials for hydrogen storage. Russian journal of general chemistry. 2007;77(4):721-39.

39. Lawson HD, Walton SP, Chan C. Metal–organic frameworks for drug delivery: A design perspective. ACS Applied materials & interfaces. 2021;13(6):7004-20.

40. Mulyati T, Ediati R, Rosyidah A. Influence of solvothermal temperatures and times on crystallinity and morphology of MOF-5. Indonesian journal of chemistry. 2015;15(2):101-7.

41. Al Haydar M, Abid HR, Sunderland B, Wang S. Metal organic frameworks as a drug delivery system for flurbiprofen. Drug design, development and therapy. 2017;11:2685-95.

42. Chen G, Luo J, Cai M, Qin L, Wang Y, Gao L, et al. Investigation of metal-organic framework-5 (MOF-5) as an antitumor drug oridonin sustained release carrier. Molecules (Basel, Switzerland). 2019;24(18):3369-86.

43. Rowe RC, Sheskey PJ, Owen SC. Handbook of pharmaceutical excipients. 6th edition ed. London, United Kingdom: Pharmaceutical Press; 2009.

تحسين الذوبانية والانحلالية للنيكلوساميد باستخدام الهيكل الفلزي العضوي ٥ (موف-٥)

حيدر يحيى منصور الجرشه[١] و موفق محمد غريب*[١]

[١]فرع الصيدلانيات، كلية الصيدلة، جامعة بغداد، بغداد، العراق.

الخلاصة

في هذه الدراسة تم استكشاف الهيكل الفلزي العضوي ٥ (موف-٥) لتحسين ذوبانية وانحلالية عقار نيكلوساميد. تم تصنيع موف-٥ باستخدام الطريقة المحلولية الحرارية وتم تحميل نيكلوساميد فيه (نيكلوساميد@موف-٥). تم تحديد الخصائص باستخدام التقنيات التالية: المجهر الإلكتروني الماسح للانبعاثات الميدانية، وتقنية حيود الأشعة السينية، وفحص تحويل فورييه الطيفي بالأشعة تحت الحمراء، ومساحة السطح بروناور-إميت-تيلر، ومطيافية تشتت الطاقة بالأشعة السينية. تم دراسة تأثير وقت التحميل على نسبة كفاءة الانحباس والقدرة على التحميل. تم دراسة تأثير تحميل عقار نيكلوساميد داخل موف-٥ على الذوبانية والانحلالية للعقار في ثلاث وسائط مختلفة: محلول وسط حمضي ذو رقم هيدروجيني ١,٢، والماء المنزوع الايونات ذو الرقم الهيدروجيني ٦,٢، ومحلول الفوسفات المنظم ذو الرقم الهيدروجيني ٧,٤. اظهرت النائج تحسن ذوبانية عقار نيكلوساميد بشكل ملحوظ بعد ادخالها في موف-٥ في جميع الوسائط. في محلول الوسط الحمضي ذو الرقم الهيدروجيني ١,٢ تحسنت الذوبانية بمقدار ٣,٤ مرات (٦٣, ١٠ ± ٠٤, ١ ميكروغرام/مل مقارنة بـ ١٧, ٣ ± ٥٥, ٠ ميكروغرام/مل). في الماء المنزوع الايونات ذو الرقم الهيدروجيني ٦,٢ تحسنت الذوبانية بمقدار ٧, ٤ مرة (٣٧, ٦٠ ± ٧٤, ٤ ميكروغرام/مل مقارنة بـ ٨٣, ١٢ ± ٧٦, ١ ميكروغرام/مل). كان اكبر مقدار لتحسين الذوبانية في محلول الفوسفات المنظم ذو الرقم الهيدروجيني٧,٤ حيث تحسنت الذوبانية ٦,١ مرة (٨٥, ٢٠٩ ± ٧٧, ٩ ميكروغرام/مل مقارنة بـ ٥, ٣٤ ± ٦٦, ١ ميكروغرام/مل). بالنسبة للانحلالية، كانت كمية الانحلال التراكمي عند اخر نقطة اعلى بشكل ملحوظ لـ نيكلوساميد@موف-٥ في جميع الوسائط الثلاثة قيد الاختبار: ٢, ٥١% ± ٥٢, ٦% مقارنة بـ ٧٧, ١٠% ± ٧٨, ١% في محلول الوسط الحمضي ذو الرقم الهيدروجيني ١,٢، و كانت ٠٩, ٥٤% ± ٨١, ١% مقارنة بـ ٤٤, ١٢% ± ٥٧, ٠% في الماء المنزوع الايونات ذو الرقم الهيدروجيني ٦,٢، وكانت ٨٧, ٨٤% ± ٩٩. ٩% مقارنة بـ ٤٨, ١٩% ± ٨٢, ١% في محلول الفوسفات المنظم ذو الرقم الهيدروجيني٧,٤. فحوصات تحديد الخصائص اثبتت هوية عقار نيكلوساميد و موف-٥ واكدت الفحوصات ايضا دخول جزيئات نيكلوساميد داخل موف-٥ وبدون حدوث اي تفاعلات ملحوظة. مما سبق يمكن استنتاج ان موف-٥ طريقة تركيب ممكنة لتحسين ذوبانية وانحلالية عقار نيكلوساميد في الوسائط الحمضية، المائية، او القاعدية.

الكلمات المفتاحية: الانحلالية، التحسين، موف-٥، نيكلوساميد، الذوبانية.